Preparation of Fe3Si/Ferrite Micro- and Nano-Powder Composite

R. Bures, M. Streckova, M. Faberova, P. Kurek

***Abstract*—**Composite material based on Fe3Si micro-particles and Mn-Zn nano-ferrite was prepared using powder metallurgy technology. The sol-gel followed by autocombustion process was used for synthesis of $Mn_{0.8}Zn_{0.2}Fe_2O_4$ ferrite. 3 wt.% of mechanically milled ferrite was mixed with Fe3Si powder alloy. Mixed micro-nano powder system was homogenized by the Resonant Acoustic Mixing using ResodynLabRAM Mixer. This non-invasive homogenization technique was used to preserve spherical morphology of Fe3Si powder particles. Uniaxial cold pressing in the closed die at pressure 600 MPa was applied to obtain a compact sample. Microwave sintering of green compact was realized at 800°C, 20 minutes, in air.

Density of the powders and composite was measured by Hepycnometry. Impulse excitation method was used to measure elastic properties of sintered composite. Mechanical properties were evaluated by measurement of transverse rupture strength (TRS) and Vickers hardness (HV). Resistivity was measured by 4 point probe method. Ferrite phase distribution in volume of the composite was documented by metallographic analysis.

It has been found that nano-ferrite particle distributed among micro- particles of Fe3Si powder alloy led to high relative density (~93%) and suitable mechanical properties (TRS >100 MPa, HV ~1GPa, E-modulus ~140 GPa) of the composite. High electric resistivity (R~6.7 ohm.cm) of prepared composite indicate their potential application as soft magnetic material at medium and high frequencies.

***Keywords*—**Micro- and nano-composite, soft magnetic materials, microwave sintering, mechanical and electric properties.

I. INTRODUCTION

MATEREIALS based on ferromagnetic powder particles surrounded by an electrical insulation are known as Soft Magnetic Composites (SMC). Different types of ferromagnetic have been used including pure iron; Fe-P, Fe-Si alloys, Fe-Ni-Co alloys up to actually the most advanced amorphous and nanocrystalline alloys. SMC's are produced by powder metallurgy (PM) technologies. Secondary phase of SMC is electrical insulation and binder phase at the same time. High resistivity implies low eddy current losses of SMC depend on effective electrical insulation. Mechanical properties depend on binder phase. Three type of secondary phase is used in SMC: a) organic compound based on thermoplastic or thermosetting resins; b) inorganic compound based on oxides or inorganic salts; c) hybrid phase based on

organic-inorganic compounds. The ideal soft magnetic material is an isotropic media with very high magnetic permeability, low coercivity and high saturation induction as well as easily shaped into three-dimensional structures as it was concluded in review work [1].

Ferrites are basic material for high frequency application. Spinel ferrites have been investigated in recent years for their useful electrical and magnetic properties and applications in information storage systems, magnetic bulk cores, magnetic fluids, microwave absorbers and medical diagnostics [2].

Secondary phase based on ferrite could be good candidate to improve functional properties of SMC. Electromagnetic properties of ferrites are very good, but mechanical properties avoid applying pure ferrites as material for structural parts. Higher values of permeability and saturation magnetization are motivation to use ferrite as secondary phase in SMC's. Compaction of powder mixtures based on progressive soft magnetic alloys and ferrite to achieve high density is task of advanced PM technologies [3]. Functional as well as mechanical properties of source powder and SMC's strongly depend on processing parameters. Microstructure and properties development of SMC is complex process influenced by pressure, temperature, time and sintering atmosphere. Size and shape of powder particles are also very important parameter [4]-[7].

Main goal of this work was to prepare composite based on soft magnetic powder alloy mixed with spinel ferrite as insulation. Investigation of microstructure and basic properties of prepared material is the subject of this work.

II. EXPERIMENTAL MATERIAL AND METHODS

Soft magnetic powder alloy Fe-3Si (FeSi) [8] supplied by Hoganas AB, Sweden was used as a composite matrix. Powder particle size of FeSi was sieve cut at-150 μm. The apparent density was 4.37 g.cm^{-3}. Soft spinel MnZn ferrite used as secondary phase was prepared using sol-gel process followed by autocombustion. The analytical pure chemicals $Mn(NO_3)_2.4H_2O$ (99%, Acros Organic), $Zn(NO_3)2.4H_2O$ (98%, Acros Organic), $Fe(NO_3)_2$ (99+%, Acros Organic) and $C_6H_8O_7.H_2O$ (99.8% CentralChem) was used to synthesize $Mn_{0.8}Zn_{0.2}Fe2O_4$ ferrite.

The resonant acoustic homogenization technique using the LabRAM mixer was used for homogenization of FeSi and ferrite powder mixture. Compaction was provided by uniaxial cold pressing at pressure 600 MPa. Green compact was heat treated by microwave sintering in air atmosphere using single mode microwave sintering equipment. Cylindrical cavity of diameter 28 mm and of height 80 mm was used.

Radovan Bures is with the Institute of Materials Research of Slovak Academy of Sciences, Kosice, Slovak republic (corresponding author phone: 421-55-7922415; fax: 421-55-7922408; e-mail: rbures@ imr.saske.sk).

Magdalena Streckova, Maria Faberova and Pavel Kurek are with the Institute of Materials Research of Slovak Academy of Sciences, Kosice, Slovak republic (e-mail: mstreckova@imr.saske.sk, mfaberova@imr.saske.sk, pkurek@imr.saske.sk).

World Academy of Science, Engineering and Technology
International Journal of Materials and Metallurgical Engineering
Vol:9, No:3, 2015

Microstructure of the materials was observed by optical microscopes (OM) Nikon SMZ-18, Eclipse MA-200 and electron microscopes (SEM) Jeol JSM 7000F and Tescan Wega3. Quantitative metallography using software ImageJ was used to measure the volume fraction of oxides. An oxide was visualized and measured in polarized light.

Powder particle size was measured by laser diffraction technique using Mastersizer 2000E. Density (D) was measured by Hepyknometry using AccuPyc II 1340.

Mechanical properties were evaluated by measurement of transverse rupture strength (TRS) and Vickers hardness (HV). Universal testing machines Tiratest2100 and hardness tester Tukon1102 were used. Young modulus (E) was measured by impulse excitation technique using Buzz-o-Sonic device and software.

III. EXPERIMENTAL PROCEDURES

A. Mn-Zn Ferrite Synthesis

The sol-gel method was used to synthesize $Mn_{0.8}Zn_{0.2}Fe_2O_4$ ferrite. The equimolar ratio of $Mn(NO_3)_2 .4 H_2O$, $Zn(NO_3)_2.4 H_2O$, $Fe(NO_3)_2$ and $C_6H_8O_7.H_2O$ was individually dissolved in distilled water, than mixed during continuous stirring at 150 rpm. The homogeneous solution was adjusted by NH_4OH to pH 6. The solution was colored to typical red color and heated at 70ºC till creation of viscous gel. The gel was immersed in appropriate high baker and continuously heated at 200ºC after 12 h. The strong exothermic reaction and self-propagating combustion process ensure transformation of xerogel to final $Mn_{0.8}Zn_{0.2}Fe_2O_4$ ferrite in very fine nano-structure.

B. Homogenization and Compaction

Micro-powder of FeSi (97 wt.%) and nano-powder of MnZn ferrite (3 wt.%) was mixed and homogenized by non-invasive technique of resonant acoustic mixing to avoid introduce additional mechanical stresses into powder alloy before compaction. Powders were dry mixed without additives. Mixed micro-nano powder is shown in Fig. 1.
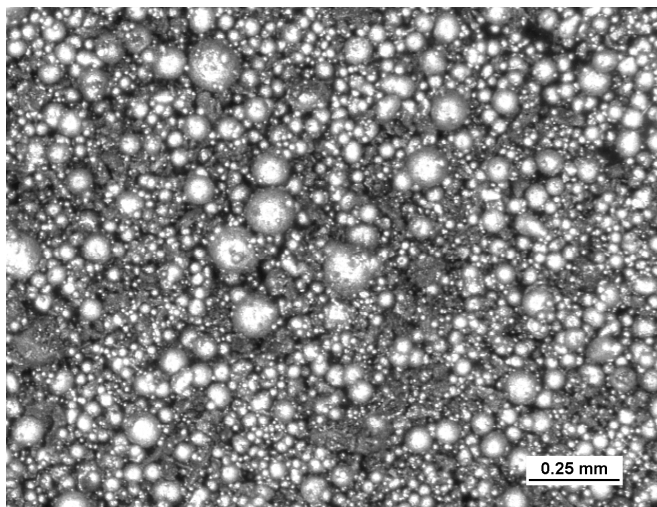

Fig. 1 Morphology of micro-nano powder mixture

The powder mixture was pressed at room temperature in cylindrical die diameter of 10 mm to sample of height about 3 mm.

Green compact was sintered by microwave heating. Temperature was measured by optical pyrometer. Absorbed microwave energy was monitored continuously by impedance analyzer to control the heating process. Profile of the time – temperature cycle and absorbed energy is shown in Fig. 2.
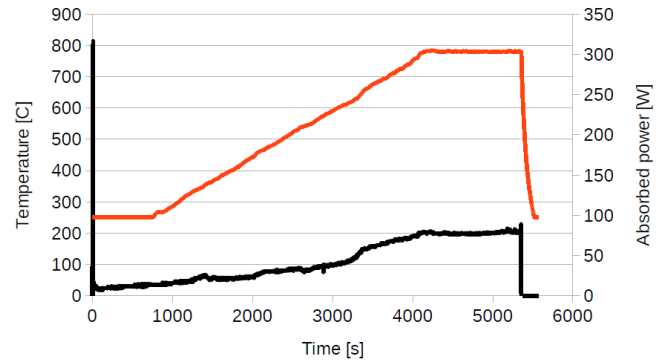

Fig. 2 Microwave sintering time-temperature and absorbed energy profile

IV. RESULTS AND DISCUSSION

A. Structure and Morphology

Spinel ferrite $Mn_{0.8}Zn_{0.2}Fe_2O_4$ prepared by auto-combustion method was milled in glass mortar. Flaky morphology of the ferrite with relative high portion of agglomeration is documented in Fig. 3.
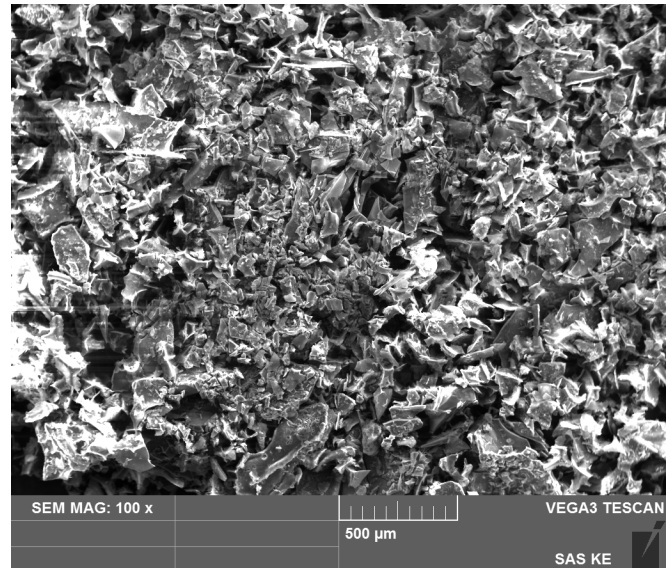

Fig. 3 SEM morphology of synthesized MnZn ferrite

Particle size measurement showed partial agglomeration of ferrite particles as it is documented in Fig. 4. Peak of the free ferrite particles is placed at size of 600 nm. Peak of size distribution of agglomerates is localized at 3.88 μm. Specific surface area of the ferrite was S=3.83 $m^2.g^{-1}$.

World Academy of Science, Engineering and Technology
International Journal of Materials and Metallurgical Engineering
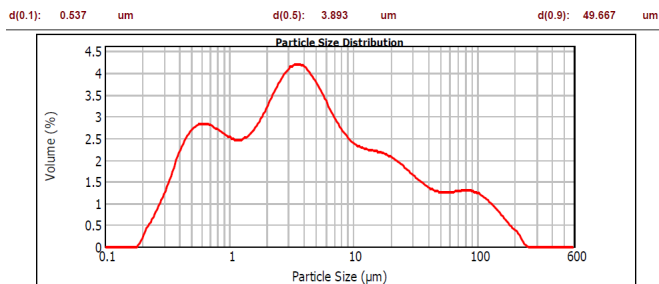Vol:9, No:3, 2015

Fig. 4 Particle size distribution of the Mn-Zn ferrite powder

Characteristic spherical morphology of FeSi atomized alloy particles is documented in Fig. 5.
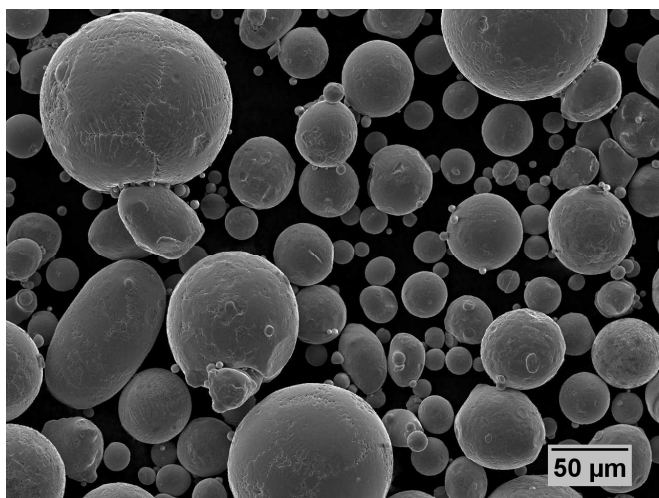

Fig. 5 SEM morphology of Fe-3Si powder alloy

FeSi particle size distribution curve is documented in Fig. 6. Mean size of FeSi particles is $d_{0.5}$=68.35 mm with specific surface area S=0.115 $m^2.g^{-1}$.
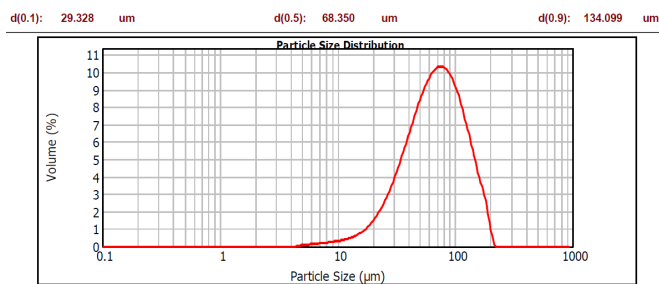

Fig. 6 Particle size distribution of the Fe-3Si powder

An agglomeration of the ferrite was suppressed during resonant acoustic mixing with FeSi powder as it is shown in Fig. 7. Nano-particles of the ferrite powder were distributed preferably to the surface of FeSi micro-particles, see Fig. 8.

Investigation of the microstructure of sintered composite shows thin layer of ferrite on the surface of origin ferrite particles as it is documented in Fig. 9. Residual ferrite agglomerates were distributed to inter-particle spaces. Additional oxide formation during sintering in dry air helps to fill green porosity. FeSi particles were slightly deformed
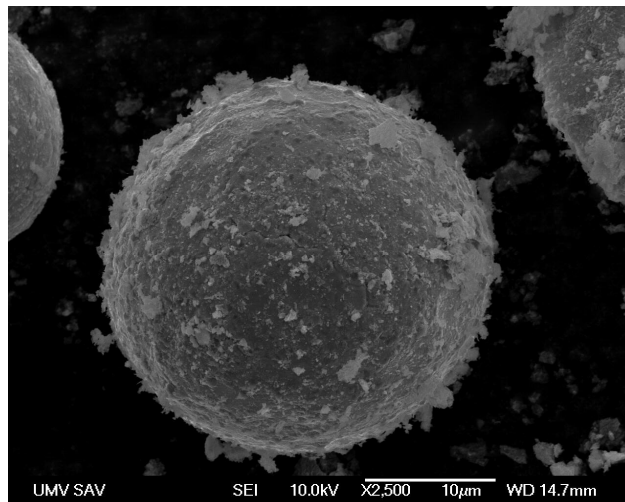
during cold pressing.

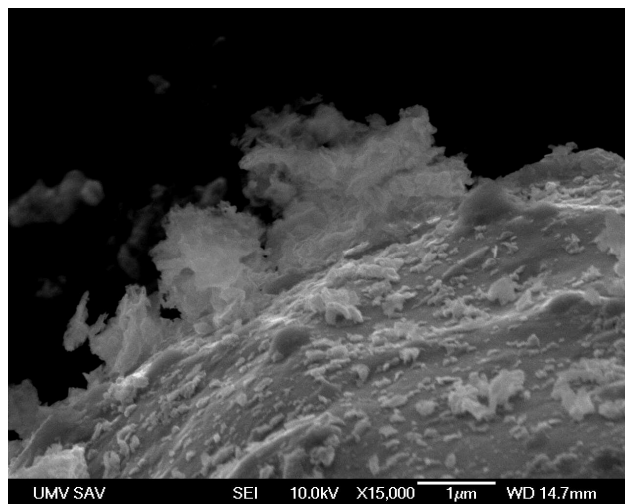Fig. 7 FeSi powder particle covered by ferrite nano-particles

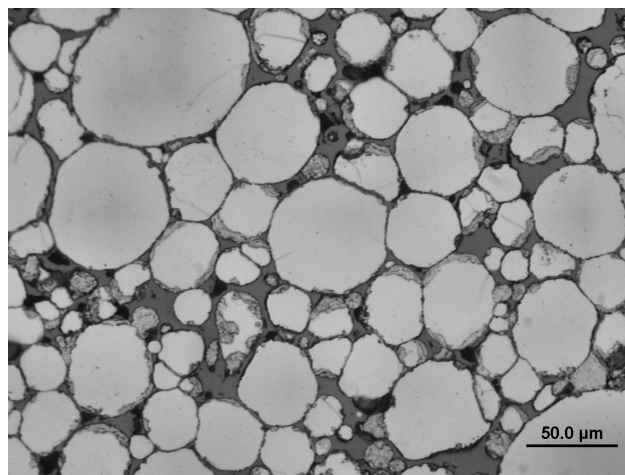
Fig. 8 Surface ofFeSi particle with ferrite nano-particles

Fig. 9 Microstructure of sintered composite (OM)

Suitable distribution of ferrite particles and small fraction of

World Academy of Science, Engineering and Technology
International Journal of Materials and Metallurgical Engineering
Vol:9, No:3, 2015

oxides, mainly SiO_2, were main mechanism of densification during sintering as indicate EDS analysis, see in Fig. 10.
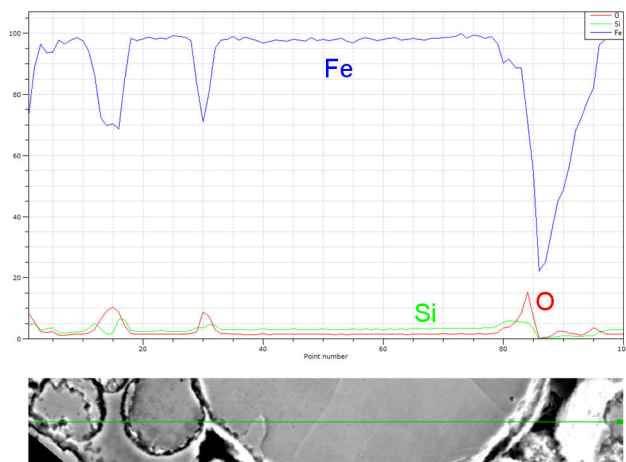

Fig. 10 EDS line analysis of FeSi-ferrite inter-particle connections

Polarized light was used for visualization of oxides and spinel ferrite in microstructure of the composite, see in Fig. 11. Quantitative metallography was applied to thresholded images and volume fraction of oxides was measured.
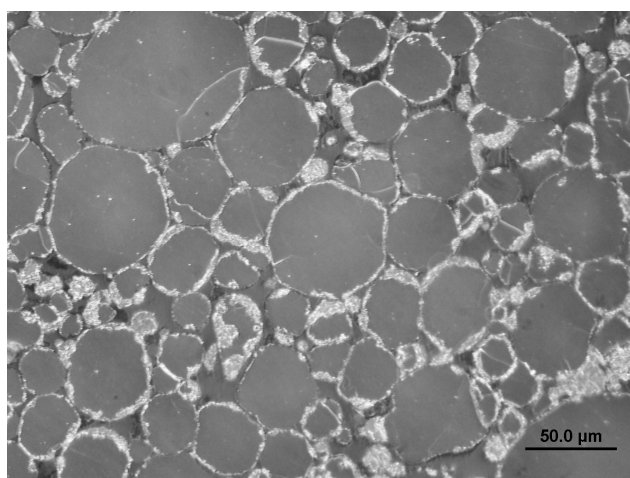

Fig. 11 Spinel ferrite and oxide visualized by polarized light

B. Properties

Density of composite, source powder and powder mixture was measured to check the densification process during composite preparation. Density values are shown in Table I.

Calculated relative density (based on size of sintered sample) of the composite is 85.13%. Measured relative density (He pyknometry) of the composite is 89.88%. Difference between total and measured density should be related to close porosity, but in this case, it is necessary to take into consider oxide formation also. Volume fraction of the oxides (based on quantitative metallography) is 10.74%. Closed porosity of the composite (calculated as difference between total porosity and porosity measured by He pyknometry) is 10.12%. Closed

porosity measured by Hepyknometry is related to volume fraction of the oxides measured by quantitative metallography. Porosity about 4 % corresponds with measured properties of the composite.

Measured properties of the composite are listed in Table II.

TABLE I
DENSITIES OF POWDER AND COMPOSITE

Material	D_{calc} [g.cm^{-3}]	D_{He} [g.cm^{-3}]	SD [g.cm^{-3}]
$Mn_{0.8}Zn_{0.2}Fe_2O_4$ nano-powder	-	3.3375	0.00224
FeSi micro-powder	-	7.4899	0.0040
FeSi-ferrite powder mixture	7.3643	7.2266	0.0061
FeSi-ferrite green compact	5.9244	6.3384	0.0081
FeSi-ferrite sintered composite	6.152	6.4951	0.0123

D_{CALC} – calculated value (based on size of cylinder sample)
D_{He} - measured by He pyknometry
SD – standard deviation of the He pyknometry measurement

TABLE II
PROPERTIES OF SINTERED COMPOSITES

Temperature °C	D gcm^{-3}	R [Ω.cm]	E [GPa]	HV [GPa]	TRS [MPa]
785	6.567	6.72	130	0.67	109
700	6.730	2.45	143	0.91	74
450	6.238	0.68	67	0.69	22

D – densitycalculated based on size of bar sample
R – resistivity Standard Deviation SD=0.285
E – Young modulus SD=0.028
HV – Vickers hardness at load 1 kgf, SD=0.045
TRS – Transverse rupture strength SD=9.91

Mechanical properties of prepared FeSi-ferrite composite are proportional to ferrite content. Values of TRS of the composites decrease with decreasing sintering temperature. Higher E modulus and hardness as well as density could indicate appropriate sinterability of the composite at 700°C, but values of strength and resistivity are weak after sintering at temperature below 785°C. Suitable mechanical and electric properties were achieved after sintering at 780°C, 20 minutes in air atmosphere. Table III shows selected properties of some MnZn ferrites and FeSi compacted materials.

TABLE III
COMPARISON OF THE PROPERTIES

Reference	material	R [Ω.cm]	E [GPa]	HV [GPa]	TRS [MPa]
Tanaka [9]	Polycrystalline MnZn ferrite	-	175-177	6.0-6.7	195-265
Matsuo [10]	MnZn ferrite grain, size 8-10 μm	-		-	60-110
Ahmed [11]	$Mn_{0.8}Zn_{0.2}Fe_2O_4$, grain size 90-115 nm	8.10^5	-	-	-
Syue [12]	$Mn_{0.8}Zn_{0.2}Fe_2O_4$, grain size 27-37 nm	3.10^6	-	-	-
Pramiz [13]	Sintered Fe-3Si	5.10^{-5}	-	-	-
Streckova [14]	Fe-3Si resin bonded	2.10^{-1}	34	0.45	97
GKN [15]	Fe-3Si sintered	-	160	0.48	-

R – resistivity Standard Deviation SD=2.525
E – Young modulus SD=0.028
HV – Vickers hardness at load 1 kgf, SD=0.045
TRS – Transverse rupture strength SD=9.91

The hardness is increased in comparison to FeSi bulk

World Academy of Science, Engineering and Technology
International Journal of Materials and Metallurgical Engineering
Vol:9, No:3, 2015

material whereas value of the strength is almost without changes. Resistivity of microwave sintered composite is significantly higher in comparison to resin bonded FeSi. The value of resistivity confirms homogeneous distribution of the insulation ferrite phase in volume of the composite. Important benefit of the microwave sintered FeSi-ferrite composite is relaxation residual stresses after sintering. Curing process of resin bonded FeSi is realized at low temperature below 200°C, that is why relaxation is no possible. In case of conventionally sintered FeSi is necessary to use longer time of sintering. Modeling the densification of FeSi published by de Castro [16] shows that, temperature 1150°C, after 60 minutes lead to suitable degree of densification with relatively small grain size. Higher temperature and longer sintering time cause inappropriate grain growth during conventional sintering. Industrial process of FeSi sintering is realized in 100 % hydrogen [15]. Microwave sintering technology gives possibility to shorten time and decrease a sintering temperature. Heat is generated within the sample during microwave sintering. Short sintering time and temperature gradient from inside to surface of the sample limited oxidation process. Certain portion of an oxides provide additional bond phase among FeSi and ferrite particles. Mechanical properties are not decreased by small fraction of oxides. Grain growth was significantly limited by low temperature of the microwave sintering at level of 800°C without negative effect on density.

V. Conclusion

Functional composite based on micrometers size powder of Fe-3Si alloy and nano-powder of $Mn_{0.8}Zn_{0.2}Fe_2O_4$ was prepared. Resonant acoustic mixing technology provided sufficient homogenization of the dry mixture. Microwave sintering technology intensified the densification process. The results indicates, that slow heating rate 10°C/min, sintering temperature 800°C in air atmosphere after 20 minutes presented suitable level of mechanical and electrical properties of the Fe-3Si/3MnZnFe$_2$O$_4$ composite.

Acknowledgment

References

[1] H. Shokrollahi, K. Janghorban, "Soft magnetic composite materials (SMCs)", *J Mat. Processing Technology*, vol. 189, pp. 1–12, 2007, doi:10.1016/j.jmatprotec.2007.02.034.
[2] D. S. Mathew, R-S. Juang, "An overview of the structure and magnetism of spinel ferrite nanoparticles and their synthesis in microemulsions", *Chemical Eng. J.*, vol. 129, pp. 51–65, 2007, doi:10.1016/j.cej.2006.11.001.
[3] M. Wang, Z. Zan, N. Deng, Z. Zhao, "Preparation of pure iron/Ni–Zn ferrite high strength soft magnetic composite by spark plasma sintering", *J Magn. Magn. Mat.*, vol. 361, pp. 166–169, 2014, http://dx.doi.org/10.1016/j.jmmm.2014.02.055.
[4] M. Anhalt, "Systematic investigation of particle size dependence of magnetic properties in soft magnetic composites", *J. Magn. Magn. Mat.*, vol. 320, pp. e366–e369, 2008, doi:10.1016/j.jmmm.2008.02.072.
[5] M. Anhalt, B. Weidenfeller, "Magnetic properties of hybrid-soft magnetic composites", *Mat. Sci. Eng. B*, vol. 162, pp. 64–67, 2009, doi:10.1016/j.mseb.2009.02.005.
[6] Y. Pittini-Yamada, E. A. Perigo, Y. de Hazan, S. Nakahara, "Permeability of hybrid soft magnetic composites", *Acta Materialia,* vol. 59, pp. 4291–4302, 2011, doi:10.1016/j.actamat.2011.03.053.
[7] R. Bures, et al., Structure and Properties of Composites Based on Mixed Morphology of Ferromagnetic Particles, *Acta Phys. Pol. A*, vol. 126, pp. 140-141, 2014, DOI: 10.12693/APhysPolA.126.140.
[8] Höganäs Sweden Datasheet Fe3Si 150, http://www.hoganas.com/en/business-areas/soft-magnetic-composites.
[9] T. Tanaka, "Young's and Shear Moduli, Hardness and Bending Strength of Polycrystalline Mn-Zn Ferrites", *Japan J. Applied Physics,* vol. 14, pp. 1897-1901, 1975.
[10] Y. Matsuo et al., "Magnetic Properties and Mechanical Strength of MnZn Ferrite", *IEEE Trans Magn*, vol. 37, pp. 2369-2372, 2001.
[11] M.A. Ahmed, et al., "The Influence of Zn2+ Ions Substitution on the Microstructure and Transport Properties of Mn-Zn Nanoferrites", *Mat. Sci. Applications*, vol. 5, pp. 932-942, 2014, http://dx.doi.org/10.4236/msa.2014.513095.
[12] M. R. Syue, F. J. Wei, Ch. S. Chou, Ch. M. Fu, Magnetic, dielectric, and complex impedance properties of nanocrystalline Mn–Zn ferrites prepared by novel combustion method, *Thin Solid Films*, vol. 519, pp. 8303–8306, 2011, http://dx.doi.org/10.1016/j.tsf.2011.04.003.
[13] http://www.pramiz.com/softm.html.
[14] M. Strečková, et al., "A comprehensive study of soft magnetic materials based on FeSi spheres and polymeric resin modified by silica nanorods", *Mat. Chem. Physics,* vol. 147, pp. 649-e660, 2014, http://dx.doi.org/10.1016/j.matchemphys.2014.06.004.
[15] http://www.gkn.com/sintermetals/capabilities/soft-magnetic-pm/process.
[16] J. A. de Castro, et al., "Modeling the Densification of FeSi Sintered Magnetic Alloys", *Mat. Sci. Forum*, vols. 727-728, pp 175-180, 2012, doi:10.4028/www.scientific.net/MSF.727-728.175